Title
THE PHOTOPRODUCTION OF no MESONS FROM HYDROGEN AND DEUTERIUM

Author
Andre, Calvin G.

Publication Date
1953-11-01

UNIVERSITY OF CALIFORNIA

Radiation Laboratory

BERKELEY, CALIFORNIA

DISCLAIMER

UCRL-2425
Unclassified-Physics Distribution

UNIVERSITY OF CALIFORNIA
Radiation Laboratory
Contract No. W-7405-eng-48

THE PHOTOPRODUCTION OF π^{o} MESONS FROM HYDROGEN AND DEUTERIUM

Calvin G. Andre'

(Thesis)

November, 1953

Berkeley, California

THE PHOTOPRODUCTION OF π^0 MESONS FROM HYDROGEN AND DEUTERIUM

TABLE OF CONTENTS

THE PHOTOPRODUCTION OF π^o MESONS FROM HYDROGEN AND DEUTERIUM

Calvin G. Andre'
(Thesis)
Radiation Laboratory, Department of Physics
University of California, Berkeley, California

November, 1953

ABSTRACT

The production of neutral pi mesons by the 325-Mev photon beam of the Berkeley synchrotron has been measured for hydrogen and deuterium at 90^o to the x-ray beam. The cross section ratio of the deuterium to that of hydrogen was obtained, $\sigma_D/\sigma_H \simeq 2$, independent of meson energy. The angular distribution of the π^o-mesons produced by 252-Mev incident photons on hydrogen was fitted to an $(a + b \sin^2 \theta)$ law giving the ratio of $b/a = 2.9 \pm 1$ (probable error). The π^o-mesons were detected by observing the decay gamma-rays in coincidence.

THE PHOTOPRODUCTION OF π^o MESONS FROM HYDROGEN AND DEUTERIUM

Calvin G. Andre'
(Thesis)

Radiation Laboratory, Department of Physics
University of California, Berkeley, California

November, 1953

INTRODUCTION

The first to observe the photoproduction of π^o mesons were Steinberger, Panofsky and Steller,[1,2] who detected the neutral mesons by observing coincidences between the two gamma-rays of the π^o decay. In their experiments they determined the energy and angular distributions of π^o's from beryllium, and the dependence of π^o production on atomic number. Some information was also obtained on the energy and angular distribution of π^o's from hydrogen. This work was followed by the experiments of Silverman and Stearns[3,4] who determined an excitation function from the photoproduction of π^o's from hydrogen by measuring the energy and angle of the recoil proton in the reaction $\gamma + p \rightarrow p' + \pi^o \rightarrow p' + 2\gamma$. The proton was detected in coincidence with one of the decay gamma-rays from the π^o meson. Cocconi and Silverman[5] obtained the angular distribution of π^o's from hydrogen and the production of deuterium by measuring the angular distribution of one of the gamma-rays of the neutral meson decay.

Goldschmidt-Clermont, Osborne, and Scott[6] investigated the photoproduction of π^o's from hydrogen by observing the range and the angle of the recoil protons in nuclear emulsions. They obtained the excitation curve and the angular distribution for the production of the neutral meson.

The experiments referred to thus far have all used x-ray beams from synchrotrons of approximately 320 Mev. An investigation of the cross section at higher energies is being made by Walker, Oakley and Tollestrup[7] who are using the 450-Mev beam of the California Institute of Technology synchrotron.

The present experiment was undertaken to investigate the cross section for the π^o production from deuterium and to obtain the angular distribution of π^o's from hydrogen. An attempt was also made to measure the ratio of σ_D/σ_H near threshold to determine, if possible, what interference effects arise between the radiated meson fields of the proton and neutron. This information would help determine the algebraic signs of the meson-nucleon coupling energy.[8] The π^o's were detected by using the gamma-gamma coincidence technique.

A comparison of the experimental results with the theoretical predictions is made in a following section.

EXPERIMENTAL PROCEDURE

Beam, Collimation and Target

The π^o mesons were produced by bombarding gaseous hydrogen or deuterium with the 325-Mev bremsstrahlung radiation of the "spread out" beam (pulse duration $\approx$ 3000 microseconds) of the Berkeley synchrotron. The bremsstrahlung beam was collimated by a 3/4-inch primary collimator at 55 inches from the electron target of the synchrotron. A one-inch secondary collimator was placed a few inches behind the primary collimator to absorb the electrons spraying from it. Each collimator was of lead, about 9 inches thick. In addition to these collimators, lead shielding was placed as necessary between the synchrotron and the gas target and counters to cut down the background. This arrangement is shown in Figure 1.

The container for the gas was the pressure target of R. S. White.[9] Figure 2 is a diagram of the target. The chamber which contained the gas was a stainless steel cylinder 2 inches in diameter and 24 inches long. This was surrounded by a liquid-nitrogen jacket and then a vacuum chamber. The total wall thickness of the target was about 120 mils of stainless steel. The end windows were about 50 mils thick. The gas was compressed to 2200 psi and kept at a temperature of -195.8°C with the liquid nitrogen. This pressure was obtained by using a pumping system shown schematically in Figure 3. In order to have a so-called "point target", 1-inch-thick lead cylinders surrounded the target except for a 2-1/4 inch gap. Actual photographs of the target in position and of the deuterium pumping system are shown in Figs. 4 and 5.

The Detection Apparatus

To detect the π^o mesons it was necessary to observe the two gamma-rays of the π^o decay in coincidence. The gamma-rays were observed by converting them into electrons which in turn were detected with scintillation counters. In a later paragraph we discuss in more detail this detection scheme, but first let us discuss the apparatus involved. Two "counter telescopes", each consisting of 1/4-inch lead converter followed by two scintillation counters, were used to detect the two gamma-rays of the π^o decay. To facilitate the placement of these telescopes, they were mounted

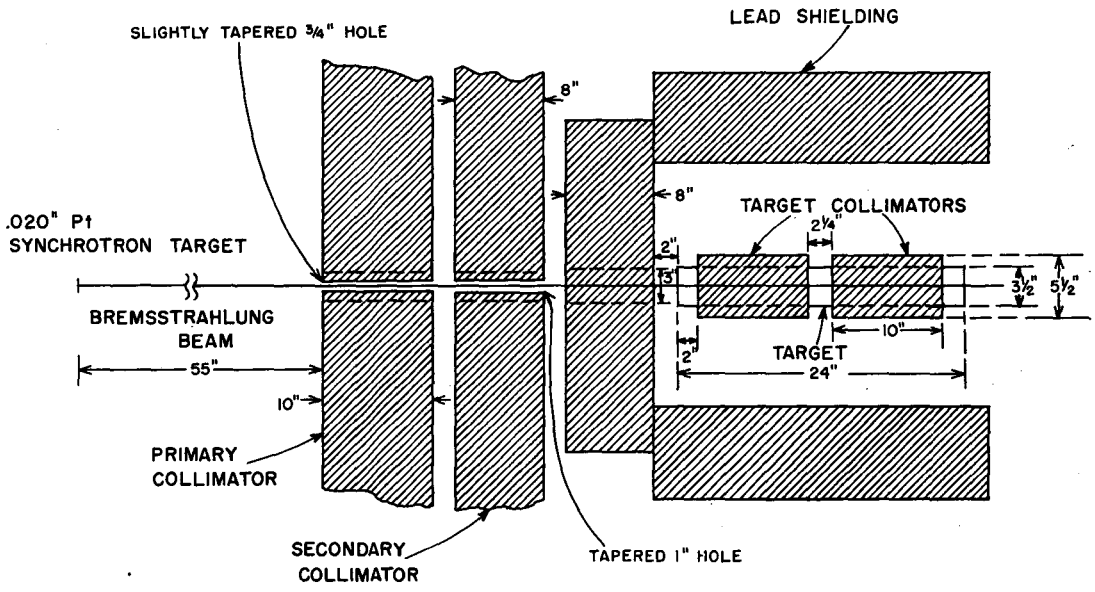

GEOMETRICAL ARRANGEMENT OF THE TARGET, COLLIMATORS AND SHIELDING

FIG. 1

MU-5934

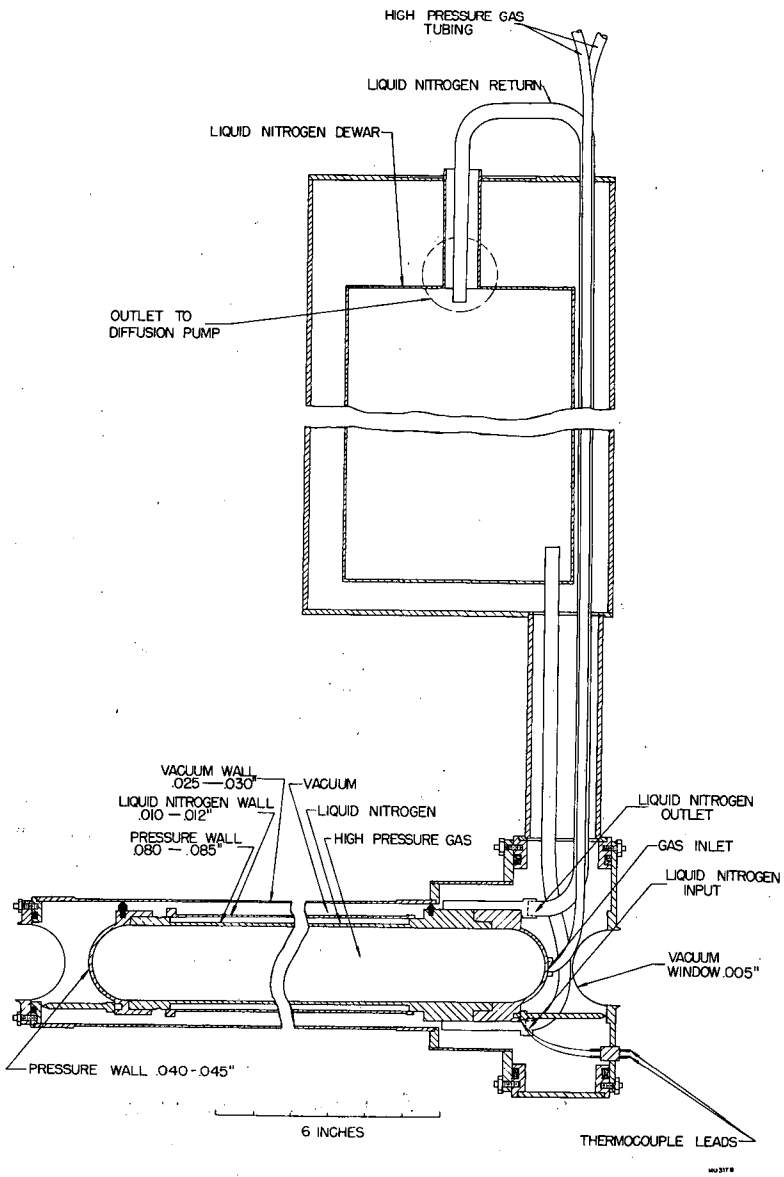

Fig. 2 The pressure target

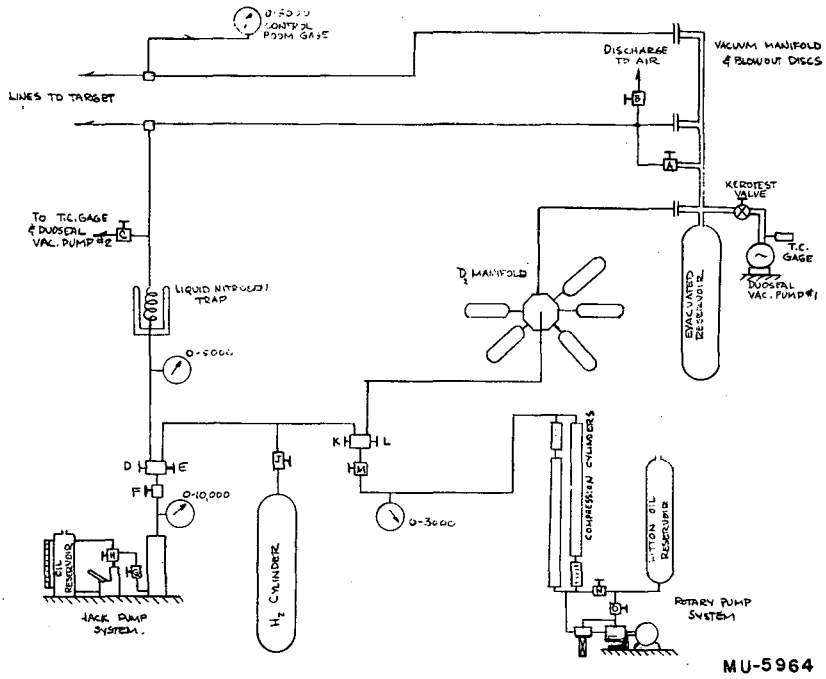

Fig. 3 Schematic diagram of the pumping system.

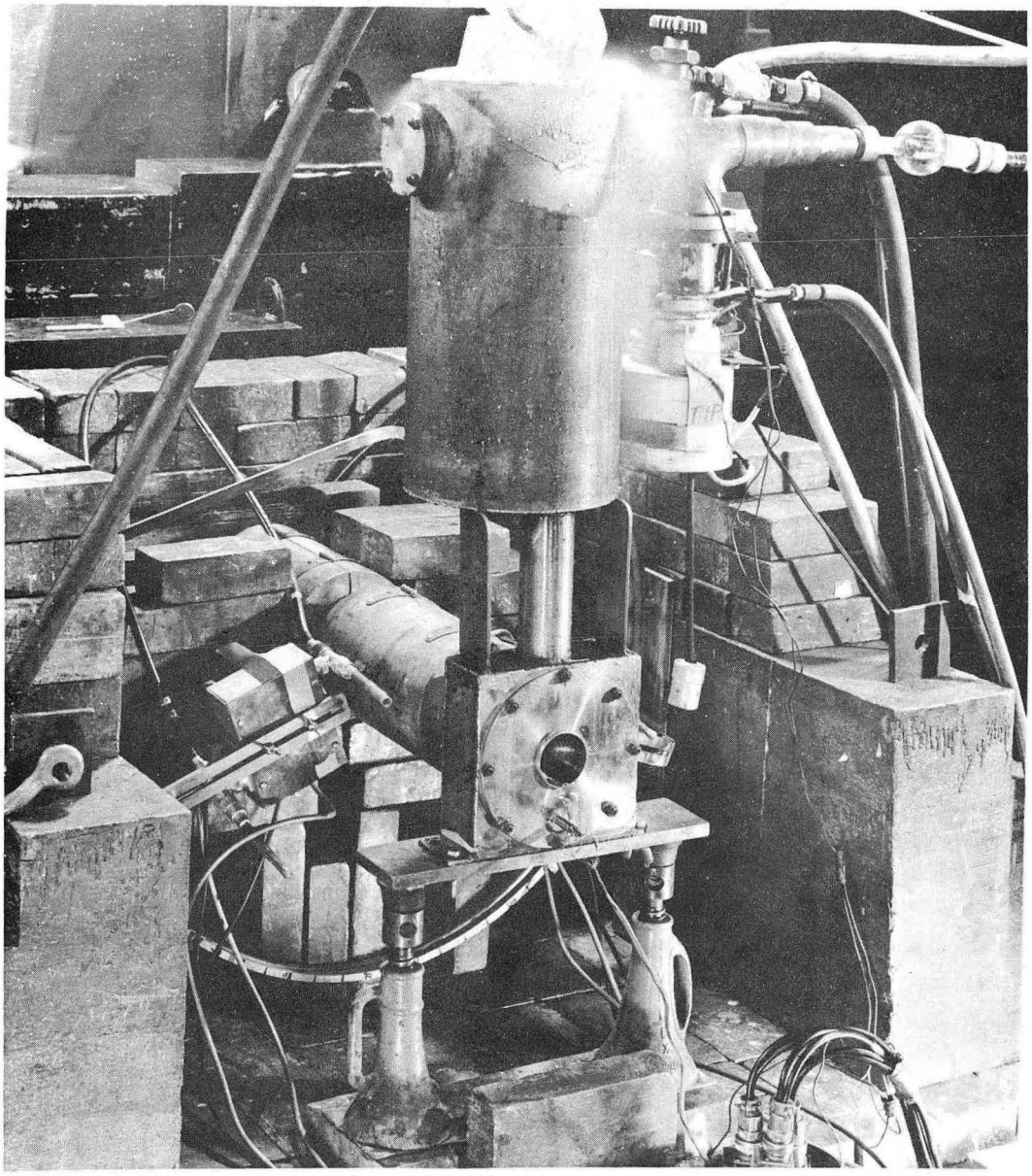

Fig. 4 Photograph of the target.

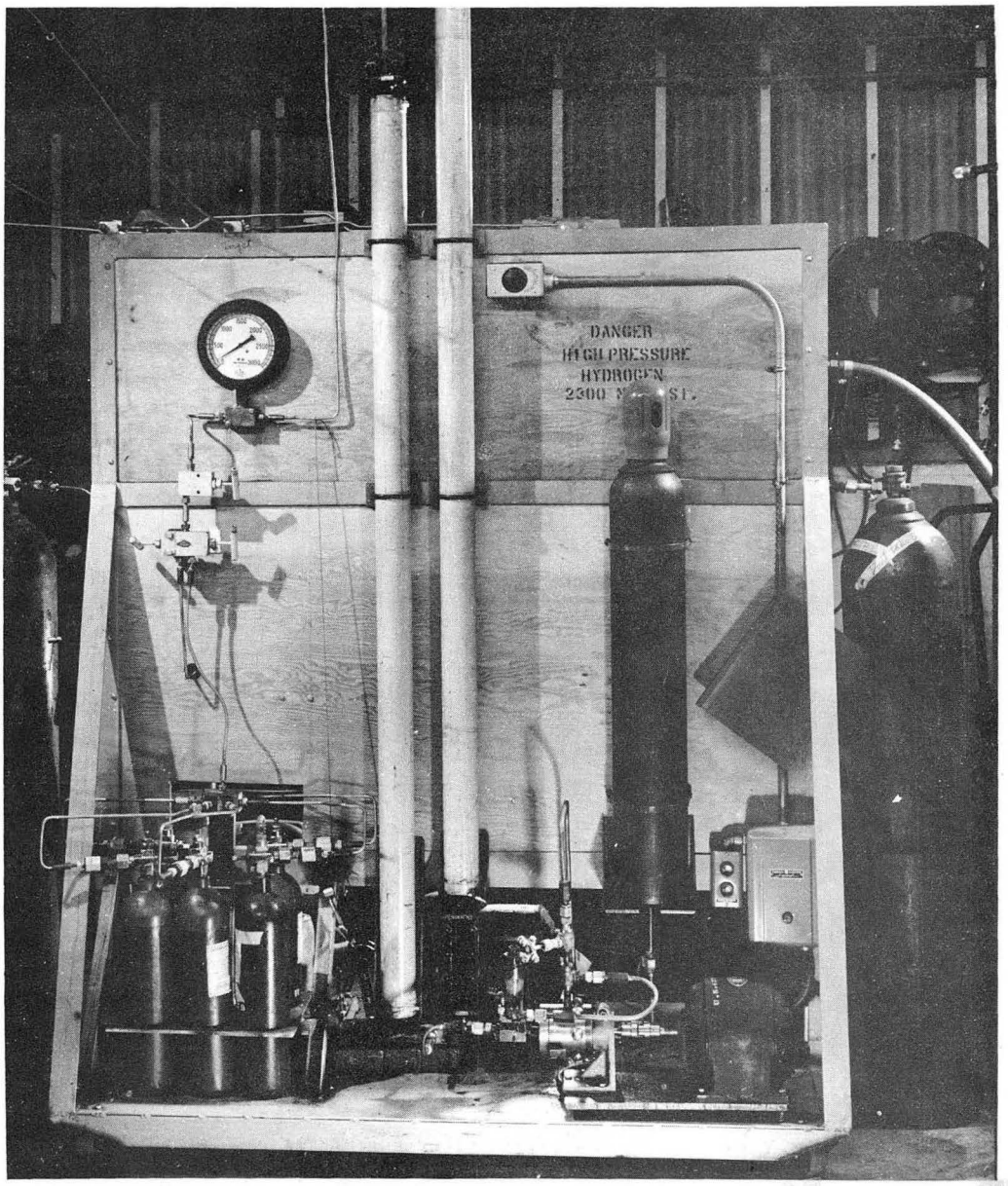

Fig. 5 Photograph of the deuterium pumping system.

on a "yoke", a semicircular frame, which was able to rotate about its diameter. Figure 6 shows the physical arrangement. With this mounting, it was possible to vary the angle between the telescopes, ϕ; the correlation angle; and also the angle the yoke made with the x-ray beam, θ, the yoke angle.

The scintillation counters were 2-1/4 in. by 2 in. by 1/4 in. stilbene crystals viewed edge on by 1P21 photomultiplier tubes. The stilbene crystals were grown by Mr. Carothers and the author.

The electronics associated with the counters is shown schematically in Figure 7. To identify a π^o decay it was necessary to establish a coincidence between the counts from the two telescopes. In order to obtain these coincidences, fast electronics (resolving time $\sim 10^{-9}$ sec) was used which was patterned after that designed by Mr. Leland Neher. The essential parts of Mr. Neher's design are a fast ($\sim 10^{-9}$ sec) limiter and the crystal diode bridge coincidence circuit with its associated preamplifier (Figs. 8 and 9). The output of each of the 1P21 photomultipliers went directly into a limiter circuit which was located in the chassis supporting each tube base. The limiter pulses were fed into the crystal diode bridge circuits. The output pulses of the bridge circuits, after going through preamplifiers in the same chassis, went into the standard UCRL linear amplifiers and then into the gate-making units, which gave microsecond gates. These gate pulses were then mixed in slow (resolving time $\sim 10^{-6}$ sec) coincidence units.

The 1P21 photomultipliers were run at a voltage of from 1500 to 1700 volts. This was necessary in order for all signals out of the photomultiplier tubes to be of sufficient amplitude so that the limiters would limit all signals to the same uniform value. This uniformity in amplitude was required for satisfactory operation of the bridge circuit. The length of the pulses -- and in turn the resolving time of the coincidence circuit -- was governed by the length of the shorting stubs attached to the limiter outputs. With 15-cm shorting stubs the resolving time was of the order of 3×10^{-9} seconds, as shown by the data recorded in Figure 10. The maximum repetition rate of the limiters was from six to ten megacycles, which placed an upper limit on the singles rates allowed in the individual counters.

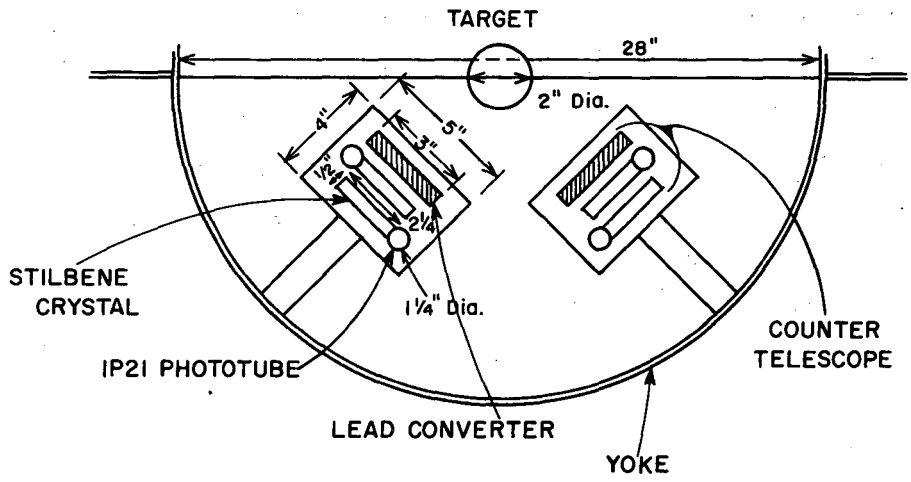

PHYSICAL ARRANGEMENT OF THE COUNTERS

FIG. 6

MU-5935

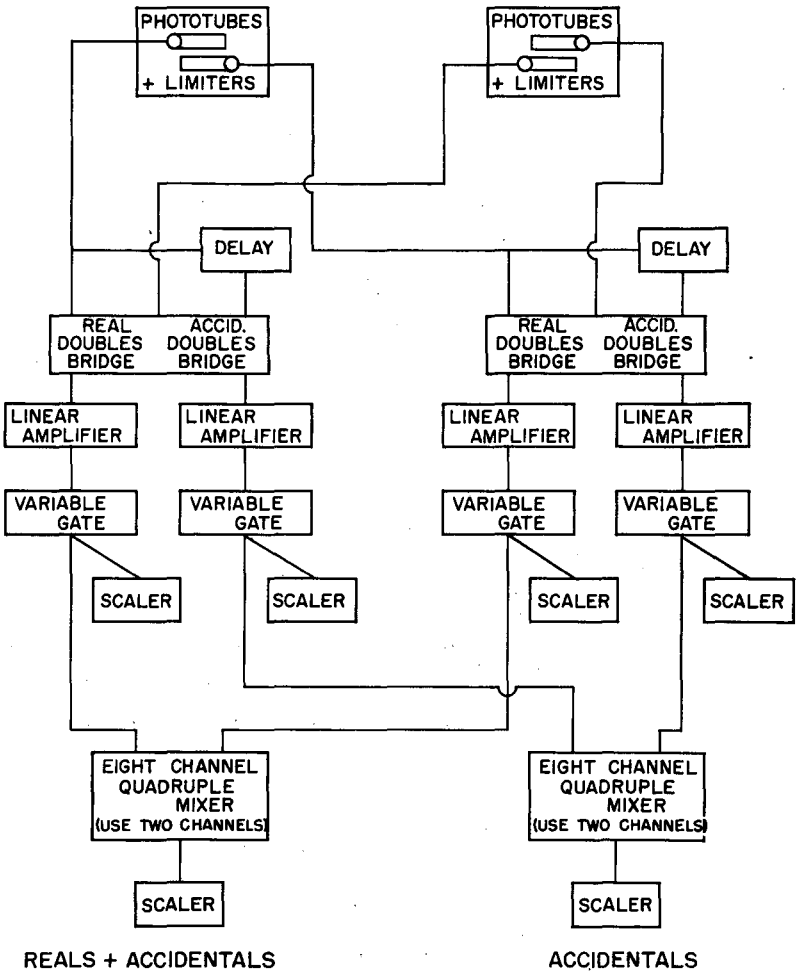

BLOCK DIAGRAM OF THE ELECTRONICS

FIG. 7

MU-5936

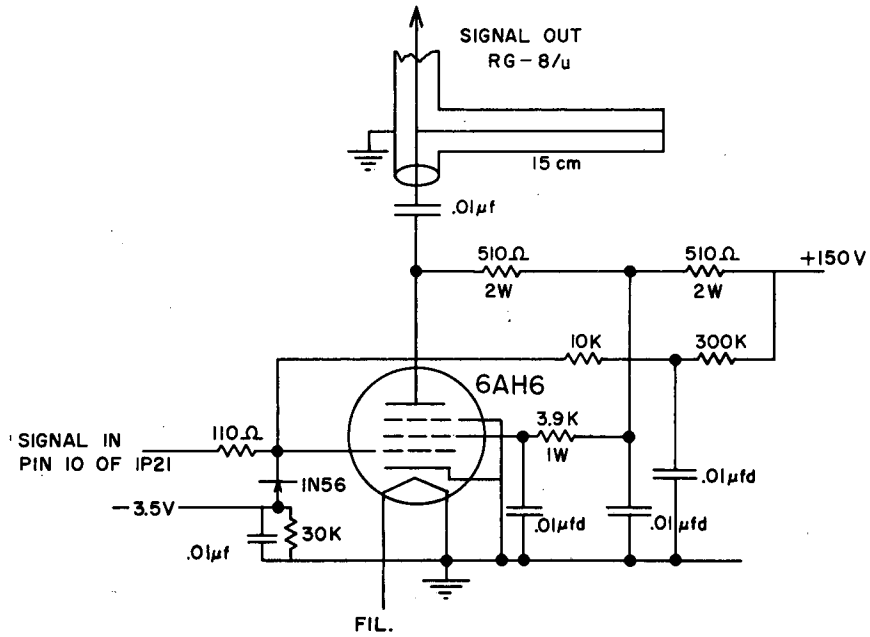

LIMITER CIRCUIT DIAGRAM

FIG. 8

MU-5937

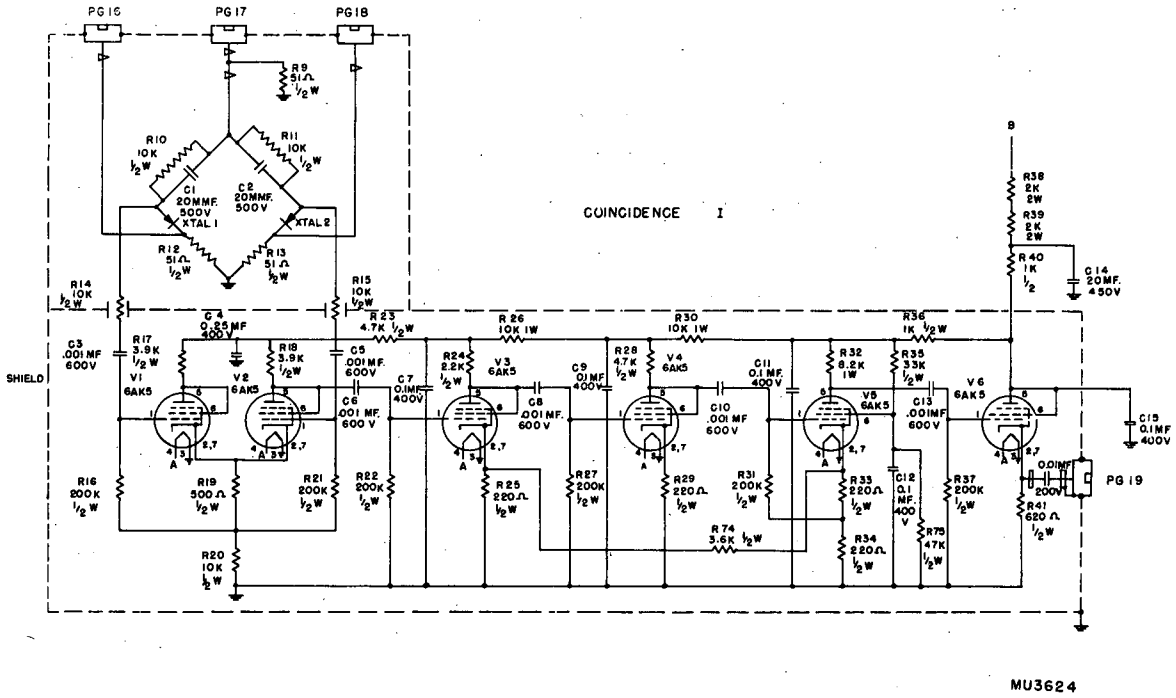

Fig. 9 Bridge and pre-amplifier circuit diagram.

The Detection Technique

As mentioned earlier, the detection of a π^o meson required that we observe the two decay gamma-rays in coincidence. In order to detect a gamma-ray with our telescope it was necessary to change the nonionizing gamma-rays into ionizing radiation. The electrons from pair production by the gamma-rays passing through a lead converter supplied this ionizing radiation. The identification of the ionizing particles as conversion electrons from gamma-rays was made by observing the counting rate as a function of the thickness of the converter and converter material. One-quarter inch of copper had the same conversion efficiency as 1/16 inch of lead. The counting rate as a function of the thickness of the lead converter is shown in Figure 11. The reason for including 2 inches of carbon while obtaining this curve was to make possible a reading for 0 lead converter. Many low-energy electrons were present, and with no lead present these electrons would tend to block the electronics. Since the radiation length of carbon is much greater than 2 inches, the effectiveness of the carbon as a converter was negligible. Under actual operation the carbon was left out as the lead itself absorbed these electrons.

The coincidences between the gamma rays were made using the electronics described in the previous section. Owing to the finite resolving time of the coincidence circuits, the observed coincidence counts consist of accidental counts in addition to true coincidences. The accidentals are due to independent events in each telescope occurring within the resolving time of the coincidence circuit. A measure of these can be made by inserting a suitable time delay in the circuit between the outputs of both the counters of one of the telescopes and their inputs to the bridge coincidence circuits. All coincidence counts obtained with this delay in the output of one of the telescopes are accidental counts. The time delay was obtained by inserting extra cable into the circuit. The amount of delay inserted was a multiple of the 47.7-megacycle rf period of the synchrotron, since the x-ray beam contains a certain amount of fine structure. We measured the accidentals at the same time we observed the real events for two reasons: the beam intensity varied

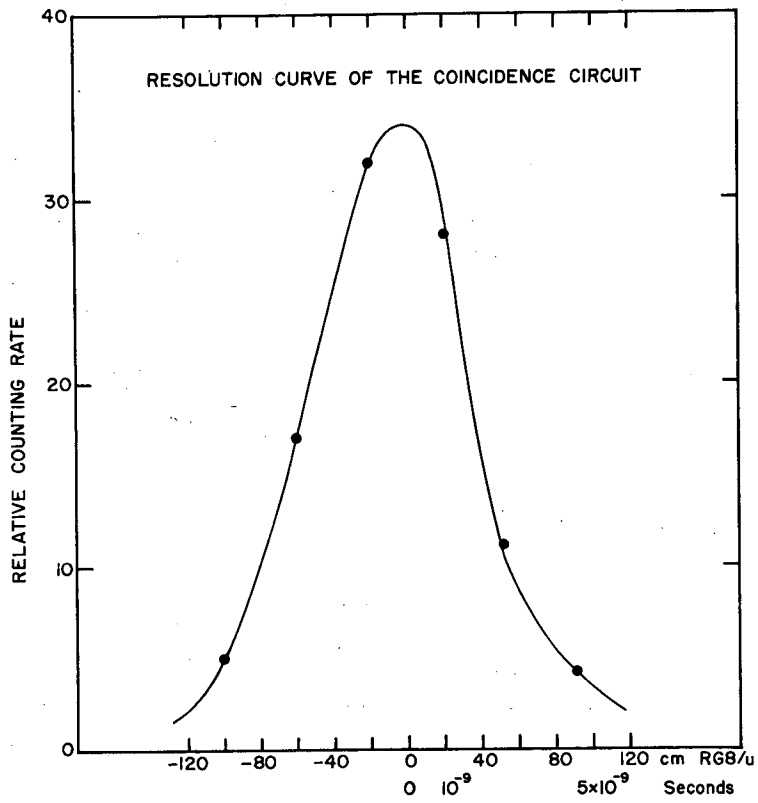

FIG. 10

MU-5938

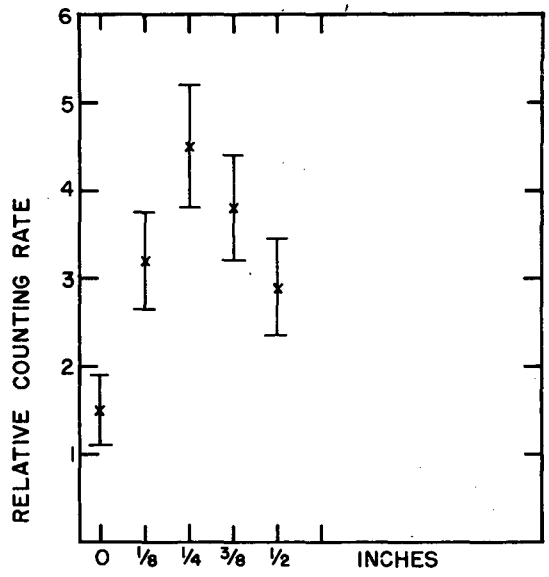

LEAD CONVERTER THICKNESS (IN ADDITION TO THE 120 MILS OF STAINLESS STEEL AND 2 INCHES OF CARBON)

TRANSITION CURVE

FIG. 11

MU-5939

erratically by a factor of ten or more during the execution of the experiment, and simultaneously measurement reduced the total amount of running time needed.

The necessity of using an anticoincidence counter in front of the lead converter to discriminate against ionizing particles was investigated. With a beryllium target, about 15 percent of the real counts were removed by using such an anticoincidence counter. Since these counts were largely due to high energy electrons, and their production varies as Z^2 of the target, it was unnecessary to use anticoincidence counters when the target was either hydrogen or deuterium.

KINEMATICS

A π^o decay is observed as a coincidence count in two telescopes that have a given orientation with respect to each other and to the x-ray beam. Figure 12 illustrates the arrangement of the telescopes. The correlation angle ϕ is the angle between the two telescopes. The yoke angle θ is the angle the plane of the telescopes makes with the x-ray beam. (The arrangment must at all times be symmetrical, i.e., the bisector of ϕ must always be perpendicular to the axis about which the yoke rotates, this axis being perpendicular to the beam.) The counting rate as a function of these angles enables us to determine the energy and angular distribution of the π^o's which are produced.

Let us designate the energy of the π^o by γ, the ratio of the total relativistic energy to the π^o rest energy. Then

$$\gamma = \left[T + (m_o c^2)_{\pi^o}\right] / (m_o c^2)_{\pi^o}.$$ In its rest frame, the π^o decays isotropically into two gamma-rays of equal energy $\frac{(m_o c^2)_{\pi^o}}{2}$ and of opposite momenta. Owing to the Doppler shift, the angle between the gamma-rays observed in the laboratory frame varies from π to $2 \sin^{-1} \gamma^{-1}$, depending on the orientation of the gamma-ray pair to the direction of the π^o motion. If the angle between the gamma-ray pair and the direction of motion of the π^o, measured in the π^o rest frame, is α, then the angle ϕ between the two gamma-rays in the laboratory is given by:

$$\sin \frac{\phi}{2} = \frac{1}{(\cos^2 \alpha + \gamma^2 \sin^2 \alpha)^{1/2}}.$$ (Derived in Appendix A)

The minimum angle ϕ_c occurs when $\alpha = 90^o$. Figure 13 shows a plot of ϕ_c vs. γ.

The probability $P(\phi)d\phi$ that the π^o gamma-ray pair subtends the angle ϕ between ϕ and $(\phi + d\phi)$ in the laboratory frame is given by:

$$P(\phi)d\phi = \frac{\sin\phi \; d\phi}{2\beta\gamma(1-\mu)^{3/2}\left[\gamma^2(1-\mu)-2\right]^{1/2}}$$

where $\beta^2 = \frac{\gamma^2 - 1}{\gamma^2}$ and $\mu = \cos\phi$. (Derived in Appendix B)

Figure 14 is a plot of $\frac{P(\phi)}{\sin\phi}$ vs. ϕ for several values of γ.

The counting rate as a function of correlation angle can now be expressed in terms of $P(\phi)d\phi$.

Let $N(\gamma)d\gamma$ be the number of π^o's of energy γ emitted per unit time perpendicular to the beam; $\Delta\Omega$, and $\Delta\Omega_2$ are the solid angles of the counters.

The counting rate $C(\phi, 90^o)$ is proportional to the number of π^o's produced, the probability of the gamma-gamma pairs subtending the particular angle ϕ and the solid angle of the counters. Summed over the energy this is then

$$C(\phi, 90^o) = 2\int_{\gamma_c}^{\gamma_{max}} P(\phi)\, d\phi\, N(\gamma)\, d\gamma \quad \frac{\Delta\Omega,\ \Delta\Omega_2}{2\pi \sin\phi\, d\phi}$$

The 2 appears here because the members of the gamma-ray pair are indistinguishable, so that the observed counts at ϕ are twice the probability $P(\phi)d\phi$ as defined in Appendix B. The term $\Delta\Omega_2$ is divided by $2\pi \sin\phi\, d\phi$ because $\Delta\Omega_2/2\pi \sin\phi\, d\phi$ is the fraction of the total solid angle between ϕ and $(\phi + d\phi)$ that the second counter sees.

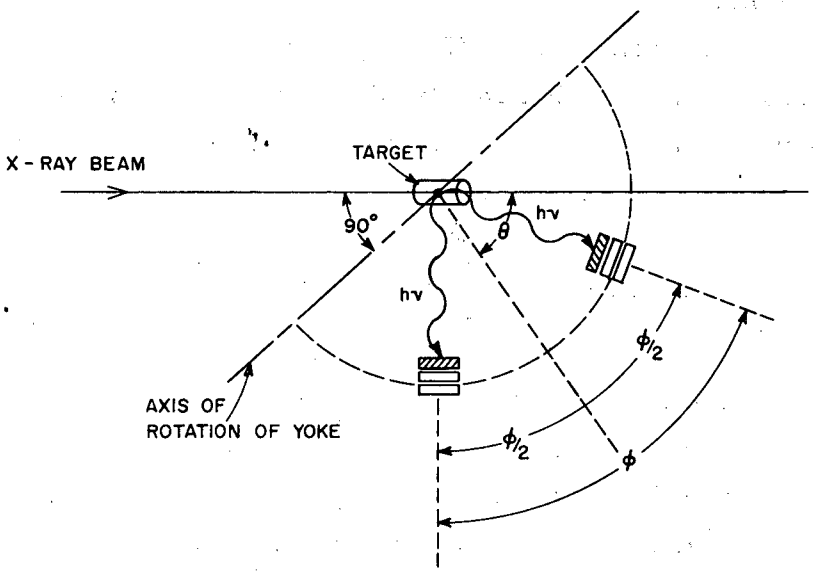

COUNTER GEOMETRY INDICATING THE "CORRELATION ANGLE" ϕ
AND THE "YOKE ANGLE" θ

FIG. 12

MU-5940

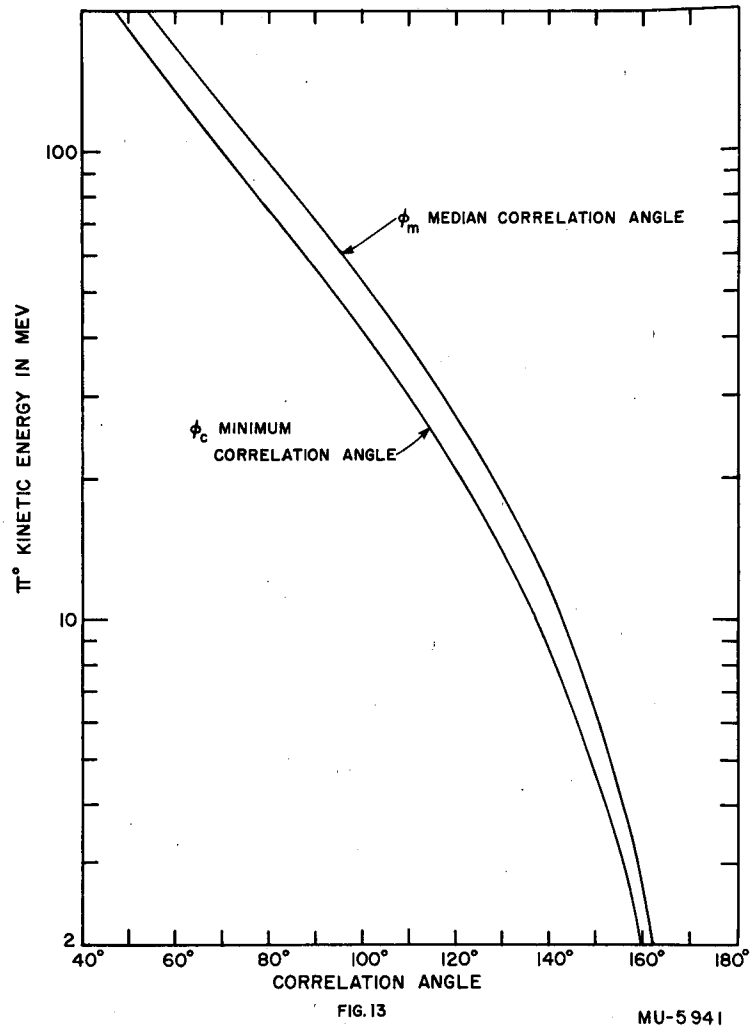

FIG. 13

Minimum and median correlation angle vs. π^o kinetic energy.

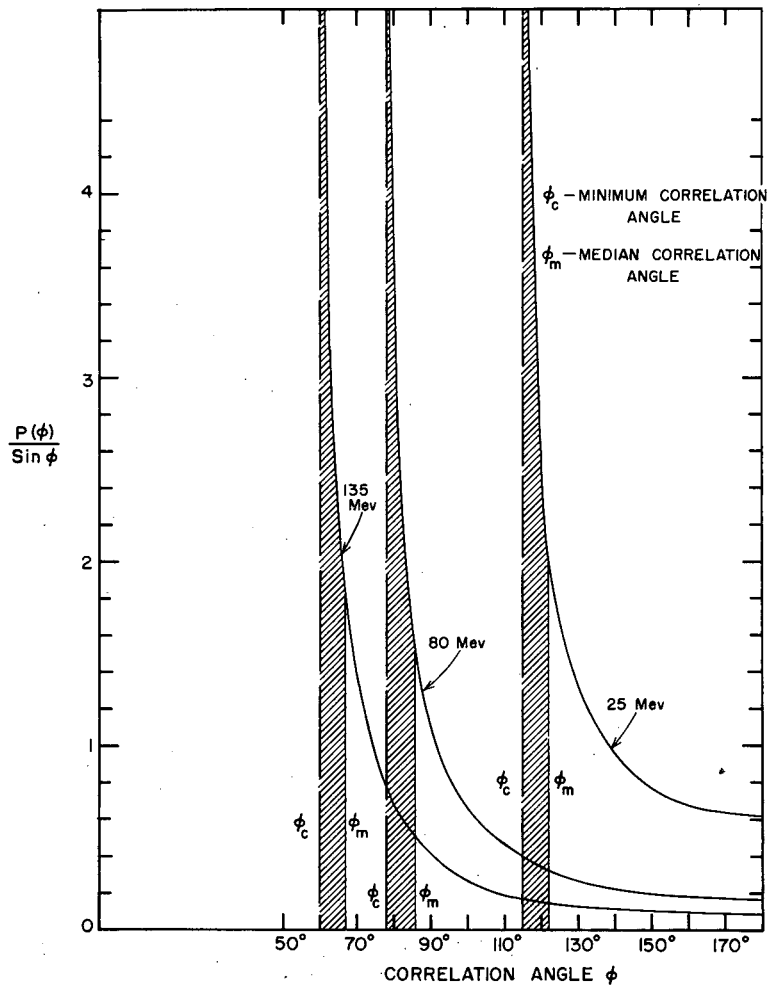

FIG. 14 MU-5942

$P(\phi)/\sin\phi$ vs. ϕ .

PROCEDURE FOR ANALYZING THE EXPERIMENTAL RESULTS

The equation

$$C(\phi, 90^{\circ}) = \int_{\gamma_c}^{\gamma_{max}} 2P(\phi)d\phi N(\gamma)d\gamma \, \Delta\Omega, \quad \frac{\Delta \Omega_2}{2\pi \sin \phi \, d\phi}$$

expresses the counting rate at ϕ in terms of the energy distribution of the π^{o}'s. To obtain the energy distribution from the observed counting rate one must either express $N(\gamma)d\gamma$ explicitly in terms of $C(\phi, 90^{\circ})$, or one can assume some arbitrary distribution for $N(\gamma)d\gamma$, perform the integration, and compare the answer with the observed values. The latter was done, and since the statistics of the observed points did not warrant a more exact expression, a step function of six steps was assumed for the energy distribution. To facilitate the computation of the integral, which is elliptic if one uses a step function for $N(\gamma)$ and integrates over the energy, we assumed a step function for the momentum distribution and integrated over the momentum. The integral can then be evaluated in closed form. The energy distribution is related to the momentum distribution by $N(\gamma) = \frac{N(P)}{\beta}$. This follows immediately from the basic relation

$$E^2 = c^2p^2 + m_o^2 c^4.$$

The evaluation of the amplitude of each step of the function was made in the following manner: The π^{o}'s in each energy interval contribute to the counting rate at each value of ϕ greater than ϕc for the lowest energy π^{o} included in that interval. The contribution is different for each value of ϕ and is determined directly by integrating the expression for $C(\phi)$. The contributions of each energy interval to the various angles ϕ are calculated in Table I. Beginning with the highest energy step one then adjusts the values of the amplitudes of the step function to best fit the experimental data.

Table I

The Relative Contributions of the Indicated π^o Energy Intervals to the Counting Rates at the Different Correlation Angles

π^o Energy Interval (Mev)	Correlation Angle ϕ					
	70^o	80^o	90^o	100^o	130^o	160^o
100.4 → 113.6	0.636	0.132	0.072	0.047	0.021	0.014
75.0 → 100.4		0.717	0.220	0.132	0.055	0.037
55.9 → 75.0			0.575	0.186	0.066	0.043
41.2 → 55.9				0.498	0.082	0.052
14.0 → 41.2					0.780	0.266
2.1 → 14.0						1.783

The procedure just outlined would give us a true energy distribution if the detection efficiency of the counter telescopes were independent of the energy of the gamma-rays. The detection efficiency is strongly energy-dependent, however. Calculations of the detection efficiency of a telescope as a function of gamma-ray energy have been made by Panofsky, Steinberger, and Steller,[2] and their results are shown in Fig. 15. Since the contribution of a high-energy π^o to a large correlation angle ϕ is possible only if α (the angle in the rest frame between the direction of the gamma-ray pair and the π^o momentum) is small, the split in energy between the two gamma-rays observed in the laboratory frame is very uneven. Therefore, it was necessary to multiply each entry in Table I by the product of the detection efficiency of each telescope for its respective gamma-ray. This was done and the results are tabulated in Table II. Table II can now be used to determine the energy distribution.

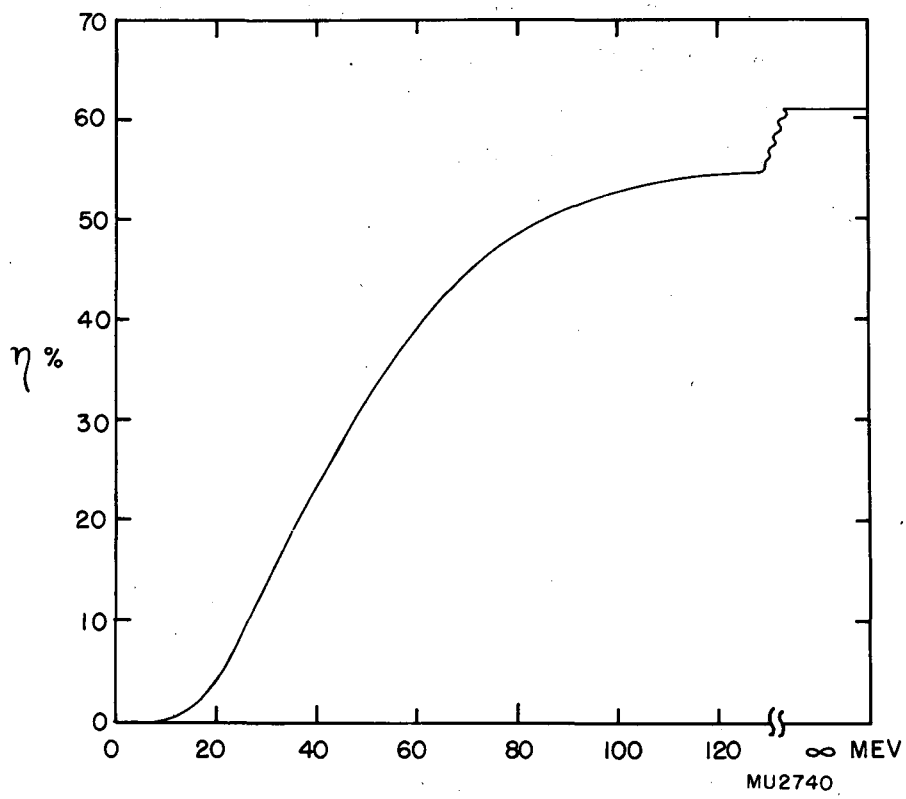

Telescope detection efficiency as a function of gamma-ray energy

Fig. 15

Table II

The Relative Contributions of the Indicated π^o Energy Intervals to the Counting Rates at the Different Correlation Angles Corrected for Telescope Efficiency

π^o Energy Interval (Mev)	Correlation Angle ϕ					
	70^o	80^o	90^o	100^o	130^o	160^o
100.4 → 113.6	0.184	0.029	0.012	0.006	0.001	0.000
75.0 → 100.4		0.186	0.044	0.020	0.004	0.002
55.9 → 75.0			0.144	0.035	0.006	0.003
41.2 → 55.9				0.115	0.010	0.004
14.0 → 41.2					0.133	0.032
2.1 → 14.0						0.303

The energy distribution thus determined gives us a cross section per "effective quantum". The number of "effective quanta" Q is given by U/k_{max} where U is the total energy of the bremsstrahlung beam and k_{max} is its upper energy limit.

To facilitate a theoretical interpretation of the results a cross section per quantum rather than per effective quantum is desired. If one can determine the energy of the x-ray that gave rise to the π^o gamma-gamma pair that was detected and if one knows the energy spectrum of the x-ray beam, the cross section per quantum can be obtained. An examination of the coefficients in Table II indicated that it was fairly reasonable to assume that there is a one-to-one correspondence between correlation angle and π^o energy. The median correlation angle for a given energy π^o is within 10^o of the minimum correlation angle for the same energy. This difference was less than the angular resolution of the telescopes, so the assumption was made that the energy of the π^o for a given correlation angle was that which would be obtained if the correlation angle were exactly the median correlation angle. As shown in Appendix B, this corresponds to an energy

$$\gamma = \left[(4 \sec^2 \phi_m/2 - 1)/3\right]^{1/2}$$

To get the differential cross section per unit solid angle per quantum the following analysis can now be made:

If $N_{\pi o}(\theta, \gamma)$ are the number of π^o's emitted per unit solid angle per unit energy interval, the counting rate for a given θ and γ would be:

$$C_{\pi o}(\theta, \gamma) = N_{\pi o}(\theta, \gamma)\ \Delta\Omega\ \Delta\Omega$$

and the cross section per unit solid angle per unit energy interval per effective quantum will be:

$$\frac{d\sigma}{d\Omega\, d\gamma} = N_{\pi o}(\theta, \gamma)\ \frac{1}{Q_{eff}\,(nt)}$$

where (nt) is the number of nuclei/cm.^{2}

The quantity $C_{\pi o}(\theta, \gamma)$ is not what is directly observed, but rather $C_p(\theta, \phi)$, the counting of gamma pairs for a given θ and ϕ. If $N_p(\theta, \phi)$ are the number of gamma pairs emitted per unit solid

angle per unit plane angle in ϕ, the counting rate for a given solid angle in θ and plane angle in ϕ is

$$C_p(\theta, \phi) = 2\, N_p(\theta, \phi)\ \frac{\Delta\Omega\, \Delta\Omega}{2\pi \sin\phi\, \Delta\phi}\ \Delta\phi\ \frac{1}{\eta^2}$$

where $\Delta\Omega/2\pi \sin\phi\, \Delta\phi$ is the fraction of the plane angle in ϕ that our second counter intercepts and η the detection efficiency of each telescope. Again the 2 is due to the indistinguishability of the two gamma-rays of the π^o decay. The cross section per unit solid angle per correlation angle interval per effective quantum will be:

$$\frac{d\sigma}{d\Omega d\phi} = \frac{C_p(\theta, \phi)}{2\ \Delta\Omega\ \frac{\Delta\Omega}{2\pi \sin\phi\, \Delta\phi}\ \Delta\phi}\ \frac{1}{Q_{eff}(nt)}\ \eta^2$$

To change this into a unit energy interval instead of a correlation angle interval one must multiply both sides by $d\phi/d\gamma$. To obtain the cross section per quantum instead of per effective quantum we must replace Q_{eff} by the number of quanta in the x-ray energy interval dk corresponding to the π^o energy interval $d\gamma$, $\frac{\Delta q}{\Delta k}\ \frac{dk}{d\gamma}$. The number of quanta in the interval $d\gamma$ is obtained by assuming a constant for the bremsstrahlung curve of $\frac{\Delta q}{\Delta k}$ vs. k. The integral

$$\int_{k=o}^{k_{max}} \frac{\Delta q}{\Delta k}\ k\, dk = \frac{\Delta q}{\Delta k}\ k\, k_{max}$$

is equal to the total energy under the curve, $Q_{eff} k_{max}$. Therefore, $\Delta q/\Delta k$ equals Q_{eff}/k. The differential cross section per unit solid angle per unit energy interval per quantum is then

$$\frac{d\sigma}{d\Omega d\gamma} = \frac{C_p(\theta, \phi)\ \frac{d\phi}{d\gamma}}{2\ \Delta\Omega\ \frac{\Delta\ \Omega\ \Delta\ \phi}{2\pi \sin\phi\, \Delta\phi}\ \frac{Q_{eff}}{k}\ \frac{dk}{d\gamma}(nt)}$$

The $\sin\phi_m \frac{d\phi_m}{d\gamma}$ can be calculated from the relationship for ϕ_m given in Appendix B; $\frac{dk}{d\gamma}$ is obtained from the expression for k in terms of π^o energy and angle. (See Appendix C.)

EXPERIMENTAL RESULTS

Energy Distribution

The production of π^o's at 90^o to the x-ray beam was measured for both hydrogen and deuterium. The counting rates as a function of the correlation angle are tabulated in Table III and are plotted in Figs. 16 and 17. The energy distributions obtained from these data (by using Table II as described in the previous section) are shown in Figs. 18 and 19. There is no significant difference between the shape of the spectrum for hydrogen and that for deuterium. The ratio of the production from deuterium to that from hydrogen at the various energies is shown in Table IV.

Excitation Function

The differential cross section per quantum can be obtained directly from the energy distribution of the preceding paragraph by taking into consideration the number of quanta per energy interval $\frac{Q_{eff}}{k} \frac{dk}{d\gamma}$. These results are shown in Table V and are plotted in Figs. 20 and 21. It was assumed that we could treat the proton and neutron of the deuterium nucleus as free nucleons and therefore use the same kinematical relationship as we did for hydrogen.

Absolute Cross Sections

A calibration of the beam of the snychrotron enables one to determine the absolute cross sections. The solid angle subtended by one of the counter telescopes was 0.086 steradians. The efficiency of the counter was taken to be $\eta = 0.5$. The target thickness was equal to the effective length of 5.7 cm, times the density of the gas (2.53×10^{22} atoms/cm^3 for hydrogen and 2.7×10^{22} atoms/cm^3 for deuterium)[10].

A numerical integration of

$$\frac{d\sigma}{d\Omega}(90^o) = \frac{1}{(\Delta\Omega)^2 (nt)\ \eta^2\ Q_{eff}} \int C_p(\theta, \phi) \sin\phi\, d\phi$$

then gives:

$$\frac{d\sigma}{d\Omega}(90^o)_H = 4.9 \times 10^{-30} \text{ cm}^2/\text{steradian/effective quantum}$$

$$\frac{d\sigma}{d\Omega}(90^o)_D = 12 \times 10^{-30} \text{ cm}^2/\text{steradian/effective quantum}$$

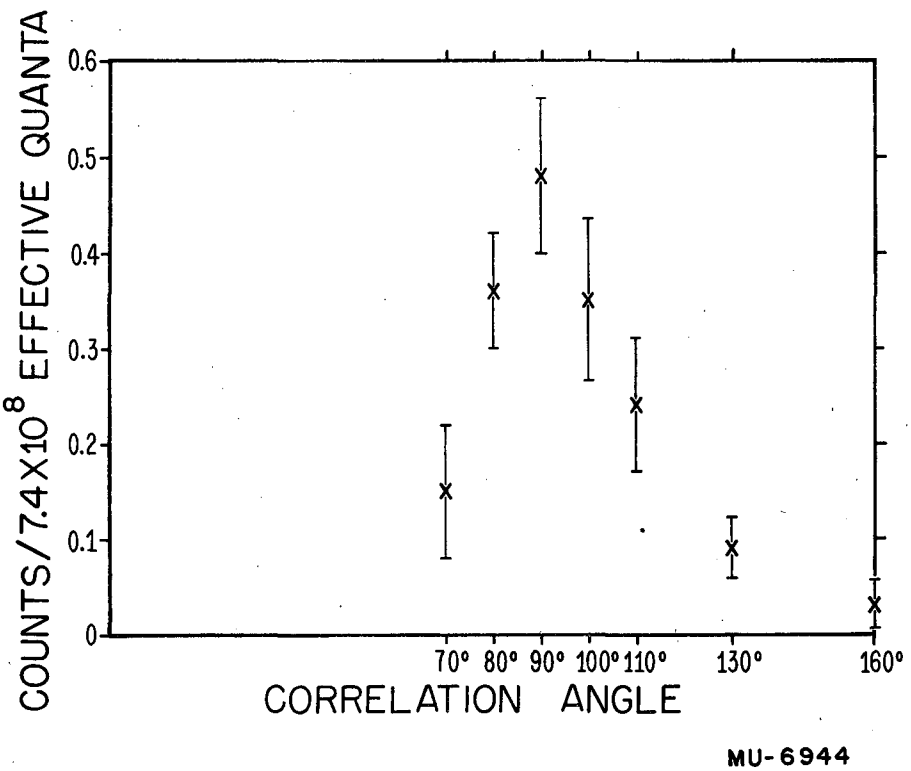

Fig. 16 Counting rate vs. correlation angle for hydrogen.

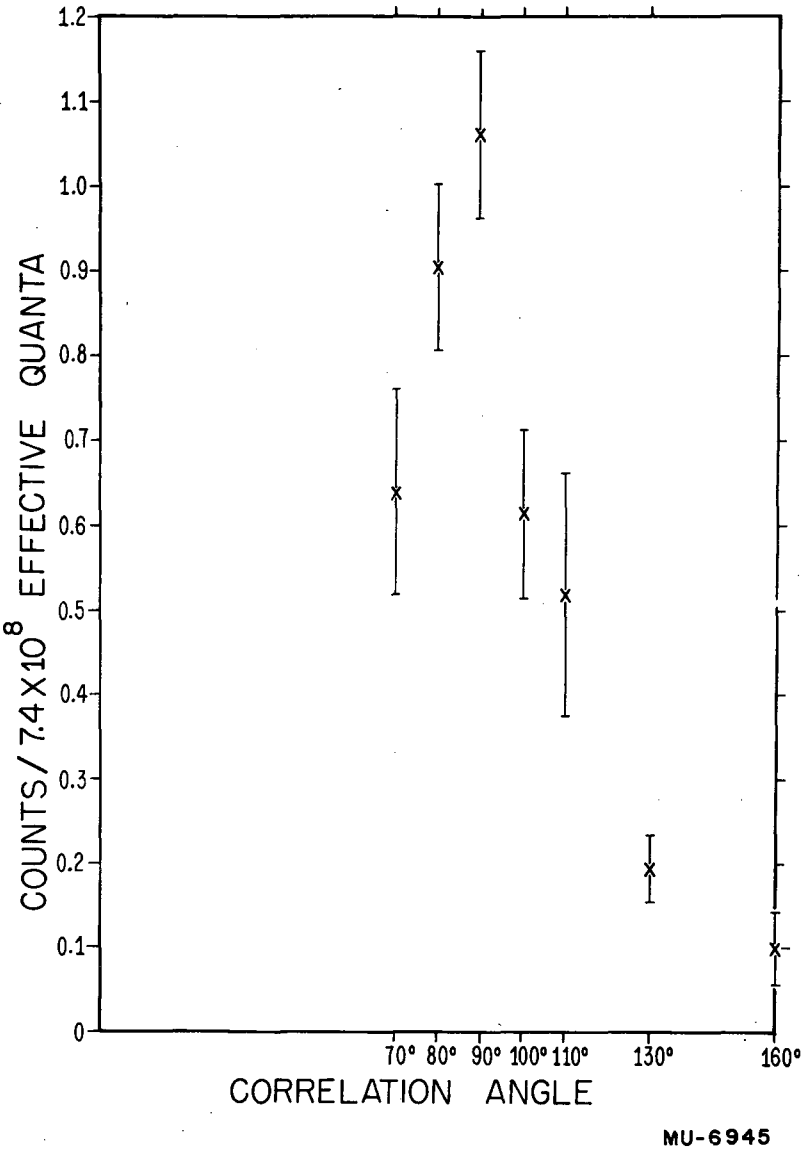

Counting rate vs. correlation angle for deuterium.

Fig. 17

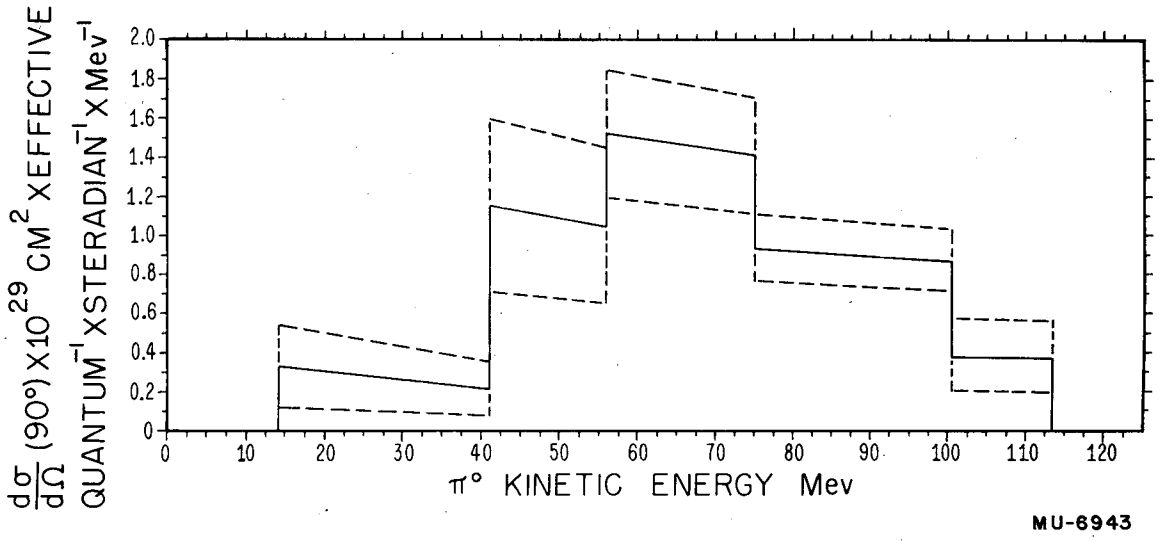

Fig. 18 Cross section for π^o production from hydrogen perpendicular to x-ray beam.

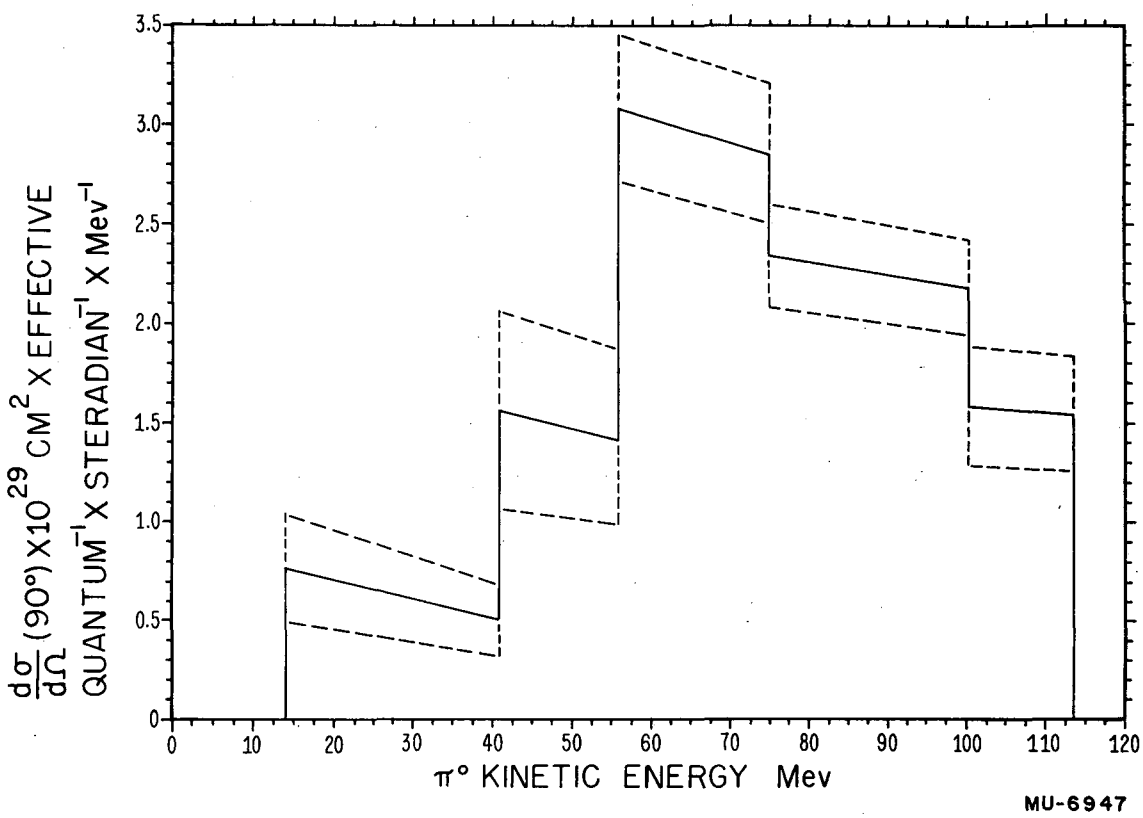

Fig. 19 Cross section for π^o production from deuterium perpendicular to x-ray beam.

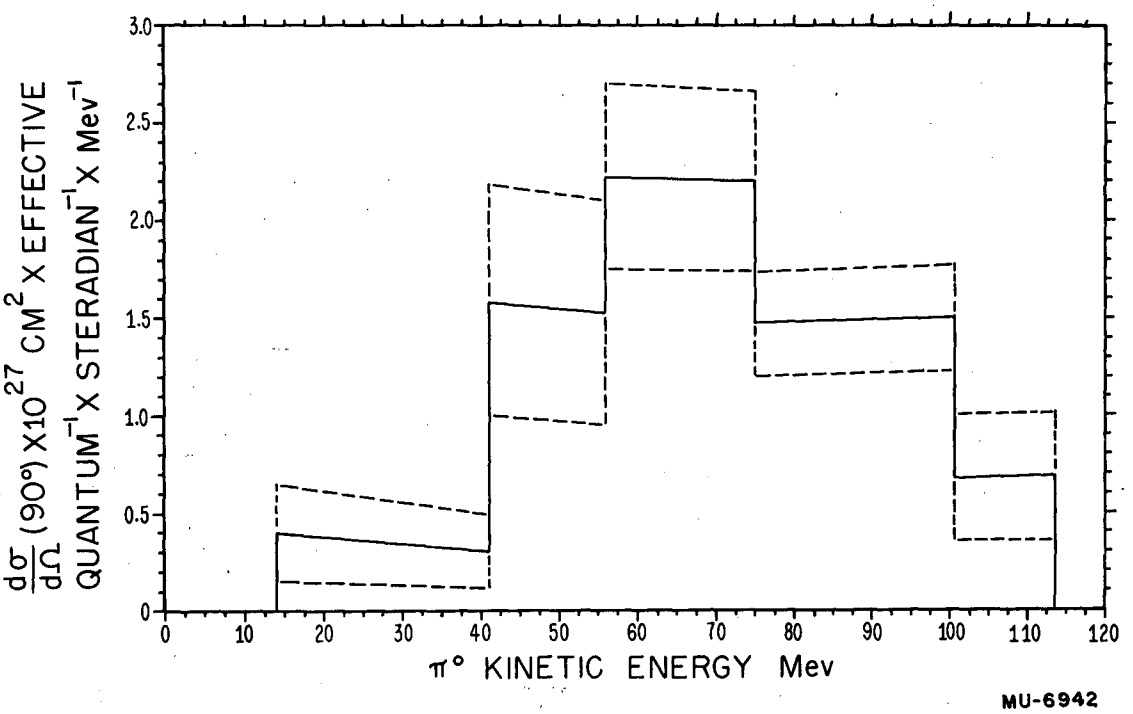

Fig. 20 Differential cross section per quantum for π° production from hydrogen at 90° (lab angle) to the x-ray beam.

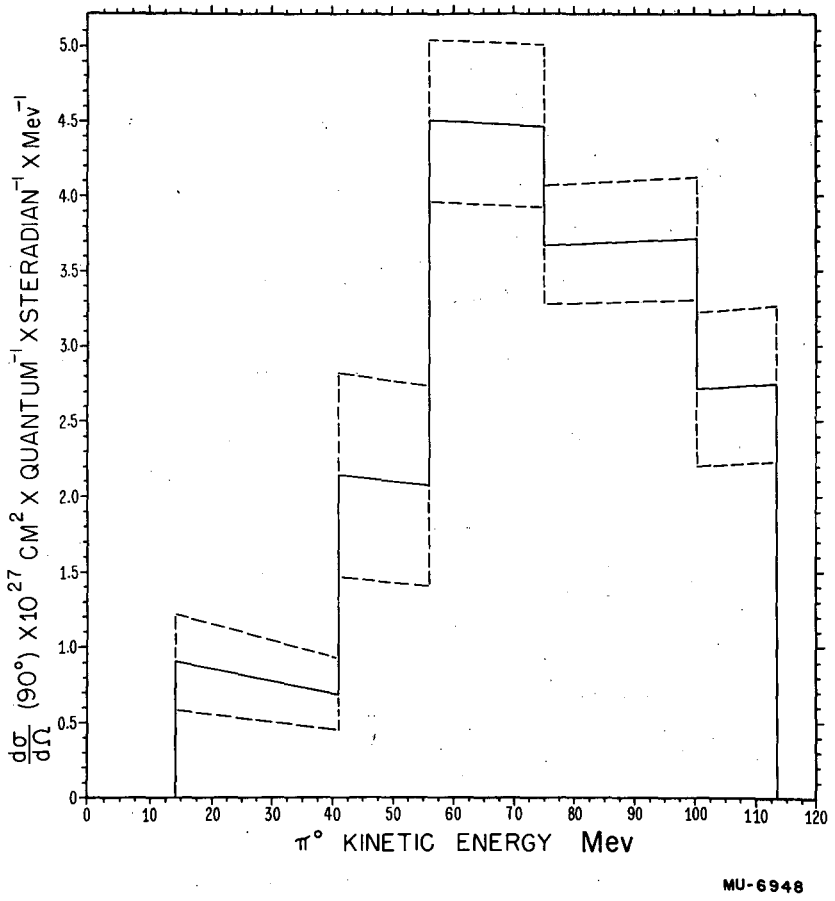

Differential cross section per quantum for π^o production from deuterium at 90^o (lab angle) to the x-ray beam.

Fig. 21

Table III

Tabulation of the Counting Rates for π^o Production from Hydrogen and Deuterium at 90^o to the X-ray Beam

Correlation Angle ϕ	Maximum Energy π^o (Mev)	Counts per 7.4×10^8 Effective Quanta	
		Hydrogen	Deuterium
70	100.4	0.15 ± 0.07	0.64 ± 0.12
80	75.0	0.36 ± 0.06	0.90 ± 0.10
90	55.9	0.48 ± 0.08	1.06 ± 0.10
100	41.2	0.35 ± 0.08	0.61 ± 0.10
110	29.8	0.24 ± 0.07	0.52 ± 0.14
130	14.0	0.09 ± 0.03	0.19 ± 0.04
160	2.1	0.03 ± 0.02	0.10 ± 0.04

Table IV

The Ratio of the Cross Sections in Deuterium and Hydrogen at $\theta = 90^{o}$ in the Laboratory System

Kinetic Energy π^{o} (Mev)	σ_D/σ_H
14	2.4 ± 1.7
41	1.4 ± 0.7
56	2.2 ± 0.5
75	2.7 ± 0.6
100	4.3 ± 2.2

Table V

The Differential Cross Section per Quantum for π^o Production from Hydrogen and Deuterium as a Function of Photon Energy

T_π (Mev)	k (Mev)	$k \frac{d\gamma}{dk}$	Hydrogen		Deuterium	
			$N_{\pi^o}(90^o, \gamma)$ x 10^{29}	$\frac{d\sigma}{d\Omega}(90^o)$ x 10^{27} per quantum	$N_{\pi^o}(90^o, \gamma)$ x 10^{29}	$\frac{d\sigma}{d\Omega}(90^o)$ x 10^{27} per quantum
113.6	325	178	0.385	0.69±0.32	1.54	2.74±0.52
→ 100.4	301	171	0.395	0.67±0.32	1.58	2.70±0.51
100.4	301	171	0.876	1.50±0.27	2.18	3.71±0.41
→ 75.0	258	157	0.936	1.47±0.26	2.34	3.67±0.40
75.0	258	157	1.40	2.20±0.46	2.85	4.46±0.54
→ 55.9	228	146	1.52	2.22±0.47	3.08	4.50±0.54
55.9	228	146	1.05	1.53±0.58	1.42	2.07±0.66
→ 41.2	205	137	1.15	1.58±0.60	1.56	2.14±0.68
41.2	205	137	0.22	0.30±0.19	0.502	0.69±0.24
→ 14.0	166	118	0.33	0.40±0.25	0.765	0.90±0.32
14.0	166	118	0.002	0.002±0.01	0.011	0.01±0.01
→ 2.1	149	110	0.005	0.006±0.02	0.027	0.03±0.03

Angular Distribution

The angular distribution of π^o production from H was obtained for a 252-Mev incident photon. This was done in the following manner: From the kinematics of a photon-nucleon collision producing a π^o, one knows the π^o energy as a function of yoke angle (Appendix C). Assuming the correspondence between π^o energy and median correlation angle mentioned earlier, the counters were set at the required correlation angles. The experimental results are shown in Table VI. The angular distribution in the center-of-mass system is readily obtained (Table VII and Appendix D) and is plotted in Fig. 22. Fitted to an $(a + b \sin^2 \bar{\theta})$ law, this gives $b/a = 2.9 \pm 1$ (probable error).

σ_D/σ_H Ratio Near Threshold

An attempt was made to measure the ratio of the cross sections for π^o production from hydrogen and deuterium just above threshold. The correlation angle used was 140^o, which corresponds to a π^o of 8.6 Mev energy. The maximum energy of the x-ray beam was lowered to 280 Mev in order to reduce the background and to keep down the production of high-energy π^o's, which contribute to the counting rate. We can consider our counts at this correlation angle as being essentially due to ~10-Mev π^o s. The results obtained are tabulated below. It was not possible to obtain better statistics since the counting rate was very low.

	Counts	Monitor Units	Counts/Monitor Unit
Hydrogen	37 ± 7.8	1556	0.024±.0.005
Deuterium	22 ± 5.1	220	0.10 ± 0.023

$$\sigma_D/\sigma_H = 4.2 \pm 1.3$$

The uncertainties assigned to the data throughout this experiment are in terms of the standard deviation.

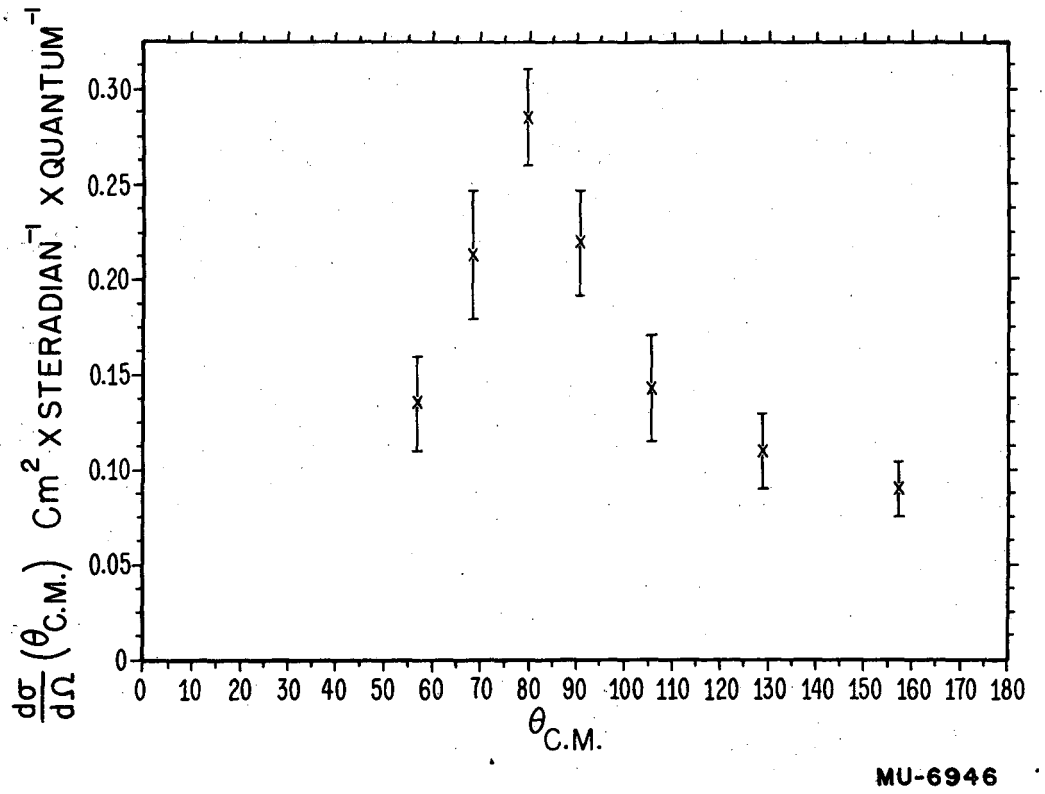

Angular distribution of π^o's from hydrogen in the center-of-mass system for a 252 Mev incident photon.

Fig. 22

Table VI

The Angular Distribution of π^o's from Hydrogen (Laboratory Angles).

θ	ϕ_m	$\sin \phi_m \frac{d\phi}{d\gamma}_m$	$\frac{d\gamma}{dk}$	$C_p(\theta, \phi)$ counts per 7.4×10^8 Effective Quanta	$\frac{d\sigma}{d\Omega}_{Lab.}$
45	78	0.798	0.863	0.279±0.052	0.192 ±0.036
55	80	0.865	0.807	0.400±0.065	0.279±0.045
65	83	0.951	0.749	0.480±0.043	0.342±0.031
75	86	1.036	0.692	0.335±0.041	0.240±0.029
90	90	1.147	0.615	0.192±0.039	0.135±0.027
115	97	1.356	0.512	0.117±0.020	0.081±0.014
150	103	1.530	0.428	0.080±0.012	0.052±0.008

Table VII

The Angular Distribution of π^o's from Hydrogen in the Center-of-Mass System

$\theta_{Lab.}$	$\frac{d\sigma}{d\Omega}_{Lab.}$	$\frac{d\cos\theta_{Lab.}}{d\cos\theta_{C.M.}}$	$\frac{d\sigma}{d\Omega}_{C.M.}$	$\theta_{C.M.}$
45	0.192±0.036	0.705	0.135 ±0.025	57
55	0.279±0.045	0.764	0.213 ±0.034	68.8
65	0.342±0.031	0.835	0.286 ±0.026	80
75	0.240±0.029	0.918	0.220 ±0.027	90.8
90	0.135±0.027	1.064	0.144 ±0.029	106
115	0.081±0.014	1.342	0.109 ±0.019	129
150	0.052±0.008	1.698	0.089 ±0.014	157.5

DISCUSSION

Some comparisons can now be made with the results of the other experiments on the photoproduction of neutral mesons. Both Silverman and Stearns[4] and Goldschmidt-Clermont, Osborne, and Scott[6], by detecting the recoil protons, have a rather direct way of determining the excitation function of the π^o production. Our experiment (detecting gamma-gamma coincidences) does not enable one to determine the details of the excitation function, but only its general shape. The results of this experiment, compared with those of Silverman and Stearns and of Goldschmidt-Clermont, Osborne, and Scott, are indicated in Figs. 23 and 24 respectively, where the dashed lines indicate the results of the other experimenters. An extension of the excitation curve to higher energies is being undertaken by Walker, Oakley, and Tollestrup.[7] Their results indicate a maximum at about 315 Mev.

The angular distribution of the π^o's has been investigated by Cocconi and Silverman[5] and also by Goldschmidt-Clermont, Osborne, and Scott.[6] Cocconi and Silverman, by observing one of the decay gamma-rays, obtained an angular distribution of the π^o's in the center-of-mass frame compatible with $a+b \cdot \sin^{2-}\theta$ where $a/b \simeq 1$. Goldschmidt-Clermont, Osborne, and Scott in fitting their data to a distribution of the same form obtained $b/a = 5 \pm 3$. The results of our experiment, fitted to an $(a+b \cdot \sin^{2-}\theta)$ law, give $b/a = 2.9 \pm 1$ (probable error).

The results of this experiment, in agreement with those of Goldschmidt-Clermont, Osborne and Scott, can be described in terms of the strong-coupling phenomenological theory of Brueckner and Watson.[11] Feld[12] has discussed this theory in the light of the results of Goldschmidt-Clermont, Osborne, and Scott. Assuming a pseudoscalar π^o meson, a magnetic dipole interaction of the gamma-ray, and an intermediate state of the nucleon with spin 3/2, the conservation laws lead to both the $p^{-3}k$ excitation curve and a $(1 + 1.5 \sin^{2-}\theta)$ angular distribution. A maximum in the excitation curve is also predicted by this theory.

The deuterium-to-hydrogen cross section was measured for various angles and energies by Cocconi and Silverman[5], and they obtained $\sigma_D \simeq 2\,\sigma_H$ independent of the energy and angle. A somewhat similar result, Table IV, was obtained in this experiment. The uncertainties in our ratios are considerably larger than theirs. These results indicate that the

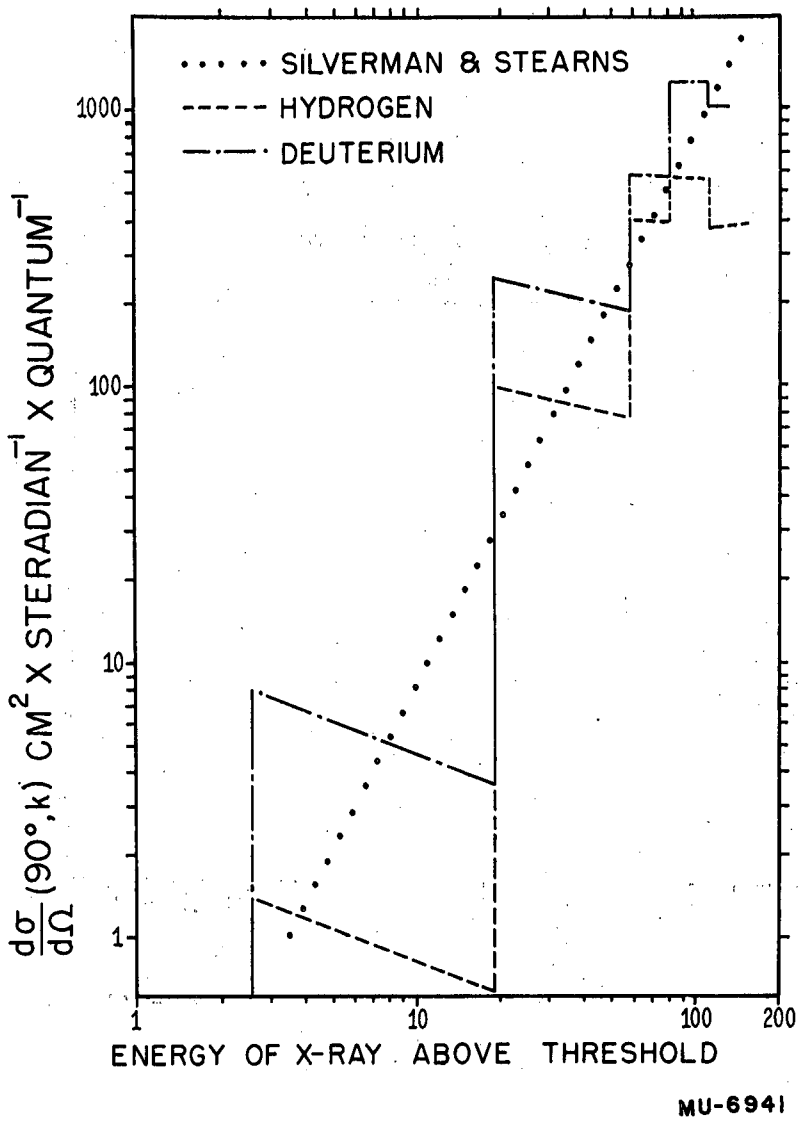

A comparison of the excitation curve of the present experiment with the results of Silverman and Stearns.

Fig. 23

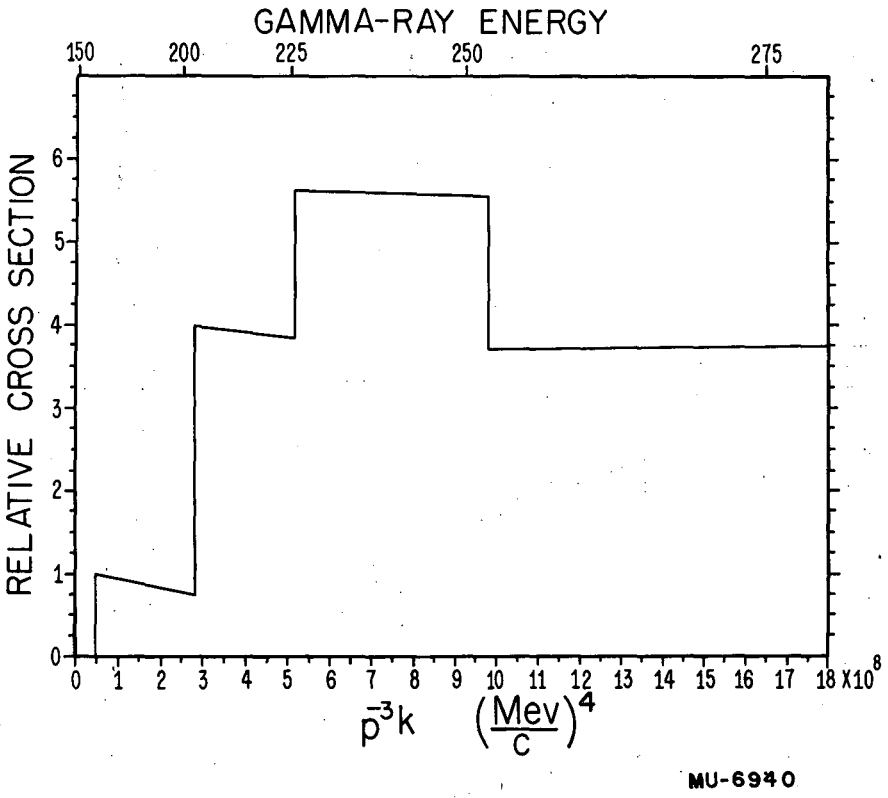

Fig. 24 The excitation curve vs $\bar{p}^{3}k$ (Momentum of meson and energy of x-ray in the center-of-mass system. Goldschmidt-Clermont, Osborne, and Scott obtained a linear dependence near threshold.)

anomalous magnetic moments of the nucleons play a role in the production of the π^o meson. It was first necessary to introduce the interaction of the photon directly with the anomalous magnetic moment of the proton in the weak-coupling theory[8] to give a cross section for π^o production that was sufficiently large. Calculations have been made by Heckrotte[8] to determine what interference effects would occur for the cases of similar or opposite signs of the coupling constant of the meson to the proton and neutron. For energies just above threshold he obtained σ_D/σ_H (signs opposite, "symmetrical theory") = 3.2; σ_D/σ_H (signs similar) = 1.09. Our results on the ratio at low energies (< 10 Mev) favor the case of opposite signs. The angular-distribution predictions of this theory, however, disagree with the experimental results in that the predictions indicate a pronounced forward distribution instead of a symmetrical one about 90^o, as obtained experimentally.

ACKNOWLEDGMENTS

I wish to express my sincere thanks to Dr. W. K. H. Panofsky for suggesting the problem, and for his continued support and guidance during the course of this work. I wish to thank Dr. H. York for his interest and helpful discussion. I am indebted to Dr. J. E. Carothers and Dr. L. Neher for their considerable assistance in all phases of this experiment. My thanks go to the synchrotron crew under Mr. George McFarland for their help in making the bombardments.

APPENDIX A

The momentum and energy of a gamma-ray are the components of a four-vector $k^i = (\vec{k}, k)$ which transforms from one frame to another frame of relative velocity β by the Lorentz transform.

The procedure is indicated.

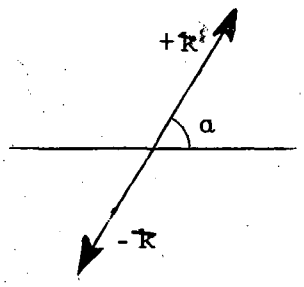

Center-of-Mass System

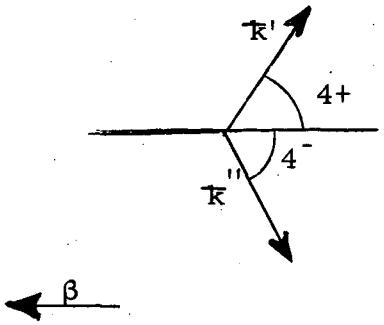

Laboratory Frame

$$(\vec{k}, k) \begin{pmatrix} \gamma & 0 & 0 & \beta\gamma \\ 0 & 1 & 0 & 0 \\ 0 & 0 & 1 & 0 \\ \beta\gamma & 0 & 0 & \gamma \end{pmatrix} = (\pm \gamma k \cos a + \beta\gamma k,\ \pm k \sin a,\ 0,\ \pm\beta\gamma k \cos a + \gamma k)$$

Therefore, $\sin 4^{\pm} = \dfrac{\pm k \sin a}{\pm \beta\gamma k \cos a + \gamma k}$, etc.

$$\sin \frac{\phi}{2} = \sin \frac{4^{+} + 4^{-}}{2} = \ldots\ldots = \frac{1}{\left[\cos^2 a + \gamma^2 \sin^2 a\right]^{1/2}}$$

APPENDIX B

$$P(\phi)d\phi = \frac{\sin\phi d\phi}{2\ \beta\gamma\ (1-\mu)^{3/2}\left[\gamma^2\ (1-\mu) - 2\right]^{1/2}}$$

can be obtained from the following considerations: In the π^o rest frame the decay gamma-rays always include the angle π, i.e., they lie along a line. We assume an isotropic distribution of the directions of this line in the π^o rest frame. The Doppler shift is different for each member of the gamma-ray pair since the one gamma-ray makes the angle α with the direction of motion as observed in the π^o rest frame, the other $\pi - \alpha$. We have the expression relating α to the angle included between the gamma-ray pair in the laboratory frame. From it we can determine the probability $P(\phi)d\phi$ that is between ϕ and $(\phi + d\phi)$, since we know the distribution of α between 0 and π. An isotropic distribution of directions in the π^o rest frame, i.e., $c\ d\ \Omega_{C.M.}$ is a $c.\sin\alpha\ d\ \alpha$ or $c.d(\cos\alpha)_{C.M.}$ distribution in α. Therefore, we can write $P(\phi)d\phi_{Lab} = 1/2\ d(\cos\alpha)_{C.M.}$. The $1/2$ arises from the normalization of the distribution of one of the gamma-rays over the sphere in the π^o rest frame.

The term $\frac{d(\cos\alpha)}{d\phi}$ is obtained from the relation

$$\sin\frac{\phi}{2} = \frac{1}{(\cos^2\alpha + \gamma^2\sin^2\alpha)^{1/2}}$$

The median angle ϕ_m is obtained by letting $\alpha = \pi/3$, since this divides the isotropic distribution in the π^o rest frame into two equal parts. Therefore, $\sin\frac{\phi m}{2} = \frac{2}{(1+3\gamma^2)^{1/2}}$

APPENDIX C

From the conservation of energy and momentum, one immediately gets:

$$k = \frac{2ME - m^2}{2\left[M - E + \cos\theta\,(T^2 + 2Tm)\right]^{1/2}}$$

where:

- k = energy of incoming photon
- M = rest energy of proton
- m = rest energy of π^o
- E = total energy of π^o
- T = kinetic energy of π^o
- θ = angle the π^o makes in the laboratory frame.

APPENDIX D

Using the Lorentz transform of the momentum four-vector, we get:

$$\cos\bar{\theta} = \frac{-\beta\bar{\gamma}^2\,\frac{\bar{E}}{\bar{p}}\sin^2\theta + \sqrt{1 - \bar{\gamma}^2\bar{\beta}^2\frac{m^2}{\bar{p}^2}\sin^2\theta}\cos\theta}{1 + \bar{\gamma}^2\bar{\beta}^2\sin^2\theta}$$

where:

- $\bar{\beta} = k/(M + k)$
- $\bar{\gamma}^2 = 1/(1 - \bar{\beta}^2)$
- $\bar{E} = (m^2 + 2Mk)/(2\sqrt{M^2 + 2Mk})$
- $\bar{E} = \bar{p}^2 + m^2$

and

- k = incident photon energy
- M = rest mass of the proton
- m, $\bar{p}$, $\bar{E}$ = the rest mass, momentum and total energy, respectively, of the π^o in the center-of-mass system
- $\bar{\theta}$ = the angle the π^o makes with the x-ray beam in the center-of-mass system
- θ = the angle the π^o makes with the x-ray beam in the laboratory system

REFERENCES

1. J. Steinberger, W. K. H. Panofsky, and J. Steller, Phys. Rev. 78, 802 (1950)
2. W. K. H. Panofsky, J. N. Steinberger, and J. Steller, Phys. Rev. 86, 180 (1952)
3. A. Silverman and M. Stearns, Phys. Rev. 83, 853 (1951)
4. A. Silverman and M. Stearns, Phys. Rev. 88, 1225 (1952)
5. G. Cocconi and A. Silverman, Phys. Rev. 88, 1230 (1952)
6. Y. Goldschmidt-Clermont, L. S. Osborne, and M. B. Scott, Phys. Rev. 89, 329 (1953).
7. R. L. Walker, D. C. Oakley, and A. V. Tollestrup, Phys. Rev. 89, 1301 (1953)
8. W. Heckrotte, L. R. Henrich, and J. V. Lepore, Phys. Rev. 85, 490 (1952); N. C. Francis and R. E. Marshak, Phys. Rev. 85, 496 (1952); and W. Heckrotte, University of California Radiation Laboratory Report No. UCRL-1868, April, 1952
9. R. S. White, M. J. Jacobson and A. G. Schulz, Phys. Rev. 88, 836 (1952)
10. Johnston, Begman, Rubin, Swanson, Corak, and Rifkin, AEC Report MDDC-850 (unpublished).
11. K. A. Brueckner and K. M. Watson, Phys. Rev. 86, 923 (1952)
12. B. T. Feld, Phys. Rev. 89, 330 (1953)